

# Part 1

## (Para)magnetic Nanoparticles: Applications in Magnetic Resonance Imaging



# 2

## MR Lymphangiography Using Nano-Sized Paramagnetic Contrast Agents with Dendrimer Cores

Hisataka Kobayashi

**Abstract:** Imaging of the lymphatic system is difficult because its channels and lymph nodes are small and not directly accessible. Currently, two clinical methods, the direct lymphangiography and the lymphoscintigraphy, are used to visualize parts of the human lymphatic system, but have significant limitations. Nano-sized contrast agents have recently been evaluated to be advantageous for visualization of the lymphatic system because of their appropriate physical sizes and the potential of signal amplification. In this review, the magnetic resonance lymphangiography using a series of nano-sized paramagnetic contrast agents, gadolinium labeled dendrimers, is discussed focusing on the synthetic method, their pharmacokinetic characteristics for selection of appropriate agents, and applications for visualization of various lymphatic disorders in mouse models.

### 2.1. Introduction

The lymphatic system is difficult to evaluate because its channels and lymph nodes are small and not directly accessible. Small animal imaging of the lymphatics would greatly further research in this field; however, the available methods are suboptimal. Two clinical methods used to visualize parts of the human lymphatic system have also been explored in mouse studies, but have significant limitations. X-ray lymphangiography uses an iodine oil agent, which must be injected directly into lymph vessels in the extremity. This requires a high degree of technical skill since lymphatic channels are difficult to cannulate in humans and it is even more challenging to perform in animals. Direct X-ray lymphangiography sometimes causes life-threatening complications including lung embolization, pulmonary edema, and adult respiratory distress syndrome if the oily iodinated contrast media intravasates into the vascular system and it has, thus, been nearly abandoned clinically (Silvestri et al., 1980). Lymphoscintigraphy is another clinical method that has been attempted

in animals. In lymphoscintigraphy, radiolabeled human serum albumin or aggregated albumin is injected intracutaneously or subcutaneously and the radiolabeled agent migrates to draining deep lymphatic vessels and nodes (Nawaz et al., 1990; Perrymore et al., 1996). While effective clinically, this method is not adequate in small animals due to the poor image resolution of radionuclide imaging.

Another approach to lymphatic imaging in animals is to employ magnetic resonance lymphangiography (MRL). Magnetic resonance imaging has the advantage of high resolution, without ionizing radiation, and has been readily adapted to small animal imaging with the use of dedicated surface coils. Individual lymphatic channels and nodes can be distinguished on MRL. A variety of MR contrast agents have been used for MRL including Gd-DTPA, liposomes, and Gd(III) macro-molecular chelates and iron oxides. Such agents have been tested in a variety of animal species including pig, rabbit, and rat models (Fujimoto et al., 2000; Harika et al., 1995; Misselwitz et al., 1999; Staatz et al., 2002).

While the study of the lymphatics in small animal models is important for research, there are few applications for direct clinical translation. Sentinel node imaging, on the other hand, has become extremely important in the surgical management of cancers, such as breast cancer and melanoma. Sentinel lymph node (SLN) biopsy has recently become a standard of care in breast cancer surgery because the disease status of the SLN accurately reflects the status of more distant axillary lymph nodes (Bass et al., 1999; Giuliano et al., 1997; Veronesi et al., 2001). The theory of sentinel node imaging is that, among all the nodes draining an organ (e.g., a breast), there is only one or at most just a few that first receive the lymphatic drainage. If the tumor has spread to the lymph nodes, it is these "sentinel" nodes that would be positive. The presence of positive sentinel nodes has implications for prognosis and management (Dowlatabadi et al., 1997; Fisher et al., 1983; Goldhirsch et al., 2001). The adoption of the sentinel node strategy has meant dramatically less invasive surgery which has gained widespread acceptance from surgeons and patients. Therefore, the testing of techniques for sentinel node imaging in small animals has recently gained attention as ways are sought to improve sentinel node imaging. Thus, by removing the SLN, the status of the entire lymphatic bed can be determined. Clinically, the two most commonly used methods employ peritumoral injections of either isosulfan blue dye or a radionuclide labeled sulfur colloid or aggregated albumin. In the "blue dye" technique, the SLN is detected by direct visualization of blue staining of the lymph node. The dye method requires dissection of tissue until the "dyed" SLN is detected. Blue dye can stain the skin for many months after injection. In lymphoscintigraphy, accumulation of the isotope, typically technetium-99m labeled sulfur colloid, can be detected with a hand held gamma counter that directs the surgeon to begin dissection in a specific region (Alazraki et al., 2000; Alazraki et al., 2001). Although lymphoscintigraphy has a limited spatial resolution, it is clinically useful. It is important to note that lymphoscintigraphy detects normal draining nodes and does not necessarily detect metastatic disease in the nodes. An alternative method that detects metastatic nodes is to

inject 2-fluoro[ $^{18}\text{F}$ ]-deoxy-D-glucose (FDG) intravenously and look for abnormal uptake in the neck and axillary regions (Guller et al., 2003). Because it is a PET emitter, FDG is harder to detect using a hand held device. Moreover, it may not detect only the SLN, since it is systemically administrated.

Experimental methods to detect sentinel nodes are being developed. When conventional low molecular weight contrast agents for MRI or CT are injected, it is not always easy to detect sentinel nodes in pig and dog models (Suga et al., 2003). However, MR lymphography performed in the pig using macromolecular contrast agents, such as Gadomer-17 or dendrimers, have been more successful (Torchia and Misselwitz, 2002; Torchia et al., 2001). A family of polymers known as dendrimers appear particularly well suited to imaging the lymphatics with MRI. Dendrimers can be synthesized to different sizes, but will remain monodispersed. Thus, a library of dendrimer-based nano-sized macromolecular paramagnetic MRI contrast agents was synthesized to investigate the best agents for MRL (Kobayashi et al., 2006; Kobayashi et al., 2003a). Herein, we describe the synthesis of dendrimer-based contrast agents and the results of preclinical studies in mouse models using these agents.

## 2.2. Preparation and Quality Control of Nano-Sized Dendrimer-Based Paramagnetic MRI Contrast Agents

The details of preparation methods for each agent have been previously published in Kobayashi et al. (2003b, 2001a,b,d). In order to load maximum gadolinium ions on a single dendrimer molecule, minor modification of reaction condition was made in each dendrimer. Other researchers used similar but different synthetic methods and chelates, and reported variable conjugation ratio of the chelate molecules and gadolinium ions to dendrimer molecules (Bryant et al., 1999; Wiener et al., 1994). All of the dendrimers investigated for MRL ranged from generation-2 (G2; 3 nm) to generation-10 (G10; 15 nm) for polyamidoamine (PAMAM) and from generation-2 to generation-4 for polypropyleneimine diaminobutane (DAB). The dendrimer substrate was obtained from commercial sources (Dendritech, Inc., Midland, MI or Aldrich Chemical Co., Milwaukee, WI). These compounds are highly soluble in aqueous solution and both possess a spherical surface topology composed of primary amino groups that increase exponentially in number with each generation (Tomalia et al., 1990; Wu et al., 1994) (Figure 2.1). The well-defined structure, monodispersity of size, and large number of available reactive surface amino groups have led to the use of dendrimers as substrates for the attachment of large numbers of chelating agents for creating macromolecular MR contrast agents (Bryant et al., 1999; Kobayashi and Brechbiel, 2003, 2004, 2005; Wiener et al., 1994). During our synthesis, dendrimers were initially concentrated in phosphate buffer at mild basic pH, and thereafter reacted with molar equivalent amounts of DTPA-derivatives as chelating moieties (Kobayashi et al., 2001d,e; Wu et al., 1994), equal to the number of surface amine residues on the dendrimer molecule and

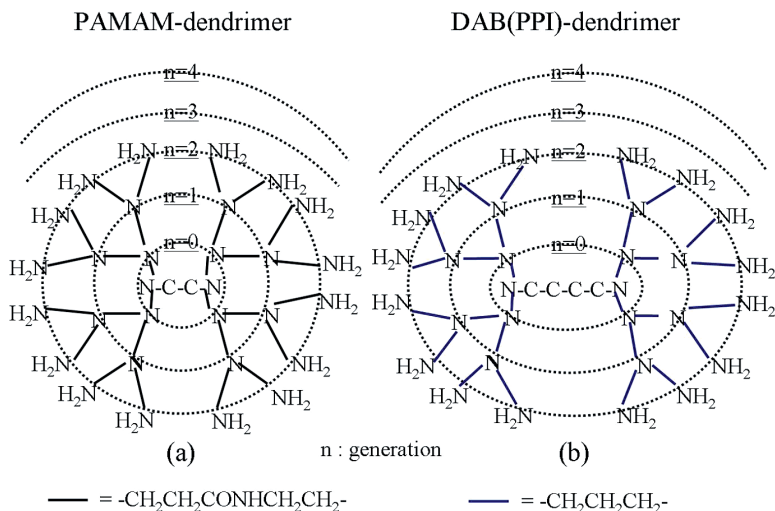


FIGURE 2.1. Schema of dendrimer cores used for contrast agents.

repeated this reaction 2 to 4 times to conjugate sufficient numbers of chelates with each dendrimer molecules. As a quality control study, a radiolabeling assay that employed either  $^{111}\text{In}$  or  $^{153}\text{Gd}$  as a tracer demonstrated the number of 1B4M-DTPA molecules conjugated to each dendrimer (Kobayashi et al., 2001e). When the reaction was stopped, more than 90% of the exterior primary amine groups on these dendrimers theoretically reacted with the 1B4M-DTPA thereby providing consistent end products suitable for animal studies (Kobayashi et al., 2001e). However, this analysis and the calculation were based on the weight of totally dehydrated and desalted chelate molecules. As a result, this HPLC-based assay may overestimate the number of chelate molecules on a dendrimer because of the water and salt content in the lyophilized chelate molecules (Kobayashi and Brechbiel, 2005).

Dendrimer-1B4M-DTPA conjugates were mixed with Gd(III) citrate at pH 4.5 and, after formation of the complex, the excess Gd(III) in each preparation was removed by diafiltration with an appropriate molecular weight filtration membrane. As a quality control, a replacement assay that employed  $^{153}\text{Gd}$  as a tracer demonstrated that the number of 1B4M-DTPA molecules of the dendrimer-1B4M-DTPA conjugates chelating Gd(III) atoms ranged from 75% to 90% (Kobayashi et al., 2001e). The larger agents generally were able to hold a smaller proportion of Gd ions. The purified contrast agents were separated by size-exclusion high performance liquid chromatography (SE-HPLC) using Sephadex series of size-exclusion columns and analyzed by the 280 nm UV absorption and  $^{153}\text{Gd}$  radioactivity. The number of Gd(III) ions per a dendrimer-based contrast agent was determined by the replacement assay and independently validated by the inductively coupled plasma mass spectrometry (ICP-MS) assay. The number of Gd(III) ions per a contrast agent was consistent on both assays (Kobayashi and Brechbiel, 2003).

The size of the dendrimer-based contrast agents were analyzed by SE-HPLC, mass spectroscopy, and light scattering methods. Although the size of the agents varied with technique, variations in size were generally small (~15%) (Kobayashi et al., 2001a; Yordanov et al., 2003).

## 2.3. MRI Methods for MR Lymphangiography

In order to test dendrimer-based MRL contrast agents in vivo, a variety of mouse models ranging from normal to diseased were evaluated. In order to perform MRL, a 1.5 T superconductive magnet unit was employed (Signa Horizon or Signa LX, Milwaukee, WI) and either a commercially available high-resolution wrist coil or dual 3 in. phased array surface coil with a custom mouse holder or a custom 1 in. bird-cage surface coil were utilized for all MRI studies to permit high-resolution images because of advantageous T1 relaxivity of dendrimer-based agents at 1.5 T and easy clinical translation. For MR lymphangiography, the T1-weighted 3D-fast spoiled gradient echo technique with fat-suppression technique and serial 3D data acquisition or 3D-fast imaging employing steady-state acquisition was used for all of the mice studied. A single MR study lasted 2–5 min and 5–10 serial studies were performed for dynamic MRL. Coronal images were usually reconstructed with 0.6–0.8 mm thick sections and 0.15–0.4 mm overlapping sections. The field of view was  $6\text{--}8 \times 3\text{--}4$  cm and the size of each voxel was therefore  $0.1\text{--}0.3 \times 0.1\text{--}0.3 \times 0.6\text{--}0.8$  mm<sup>3</sup>. Serial dynamic data were analyzed using commercially available workstations. Whole body 3D-MRIs were reconstructed with the maximum intensity projection (MIP) method to show up the enhanced lymphatic system. Details of individual experiments can be found in Kobayashi et al. (2006, 2005, 2003a,c, 2004, 2001c).

## 2.4. MR Lymphangiography with Nano-Sized Paramagnetic MRI Contrast Agent

### 2.4.1. *Optimal Size of the Agents*

In order to determine the optimal size of Gd-dendrimer for lymphatic vessel and lymph node imaging, each agent was tested in vivo. Intracutaneous injection at the phalanges revealed that larger nano-sized agents worked better for visualizing the lymphatic vessels than smaller agents. MR lymphangiograms with the largest agent studied (G8; ~13 nm) showed the best depiction of the lymphatic system among all the tested agents (Figure 2.2). The relatively large size of these molecules meant that once the agent was absorbed by the lymphatic system it tended to remain within it. In comparison, low molecular weight Gd-DTPA only faintly demonstrated the distal large lymph nodes such as the axillary and external iliac lymph nodes early after injection. In order to detect sentinel lymph nodes, various size dendrimers were tested after mammary pad injection. Among the agents tested, a G6 agent of ~10 nm in diameter proved to be the most effective (Figure 2.3). In comparison, the larger G8 dendrimer showed slower

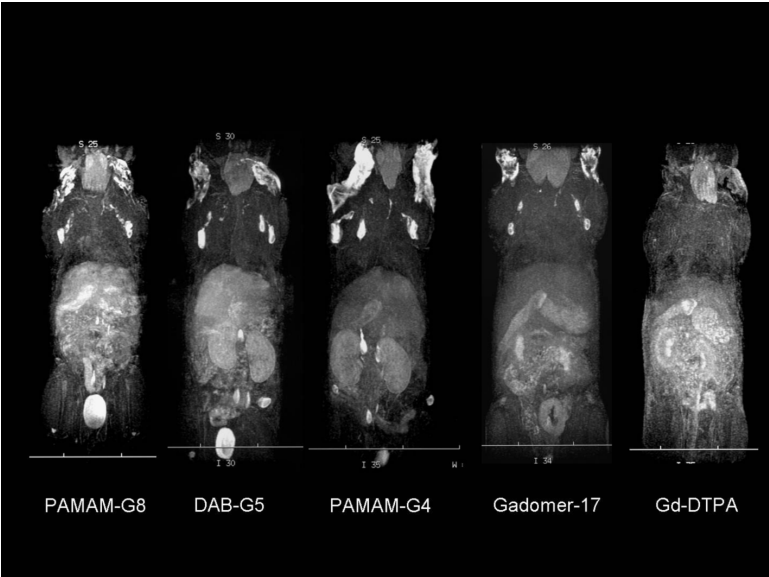


FIGURE 2.2. Whole body dynamic 3D-micro-MR lymphangiography of mice injected intracutaneously into all four middle phalanges with 0.005 mmol Gd/kg of PAMAM-G8, DAB-G5, PAMAM-G4, Gadomer-17, or Gd-DTPA are shown. The images obtained at 45 min post-injection are shown for all contrast agents tested. Maximum intensity projections are illustrated.

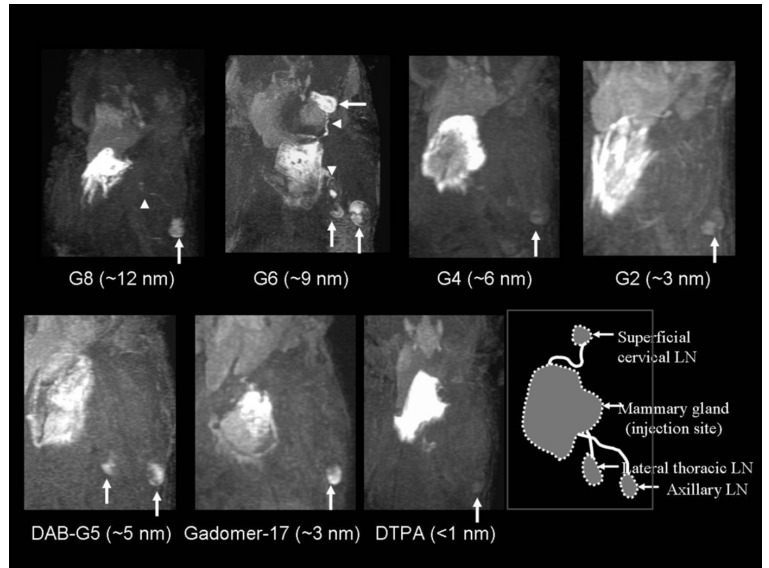


FIGURE 2.3. A series of 3D dynamic MR lymphangiograms obtained 12 min after the injection of the five contrast agents including three Gd-dendrimers. The G6 contrast agent of ~9 nm in diameter was taken up by both lymph nodes and lymphatic vessels and achieved the largest enhancement ratio among all agents examined.



enhancement of the axillary lymph node (Kobayashi et al., 2006). Smaller nano-sized agents were not as good as G6 or G8 in depicting the lymphatics and SLN. Among the smaller agents, DAB-G5 and Gadomer-17 were acceptable to visualize lymph nodes probably because of their less hydrophilic properties than PAMAM series of contrast agents (Kobayashi et al., 2006).

The ideal lymphatic imaging agent needs to be small enough to enter the lymphatic vessels, yet large enough to be retained within the lymphatics and not leak from the capillary vessels. Lymphographic contrast agents must be at least 4 nm in diameter to enable efficient retention within the lymphatics (Alazraki et al., 2001; Kobayashi et al., 2003a). Molecules smaller than 4 nm in diameter tend to diffuse into the surrounding tissue, resulting in poor signal-to-background ratios. Larger molecules, on the other hand, diffuse more slowly from the interstitial space and, thus, accumulate more slowly in the sentinel node, requiring a longer imaging window for visualizing nodes. The larger diameter G8 agent (~12 nm), used in our previous report for deep lymphatic imaging studies (Kobayashi et al., 2003c), is too large for rapid uptake by lymphatic vessels arising from the breast, although it is suitable for imaging lymphatics of the extremities. In contrast, the G6 contrast agent is retained in the lymphatic vessels, resulting in efficient enhancement of lymphatic vessels and lymph nodes. Both G2 and G4 agents were too small to stay within the lymphatic vessels, resulting in convection away from the injection site and only minimal enhancement in the lymph nodes (Figure 2.4).

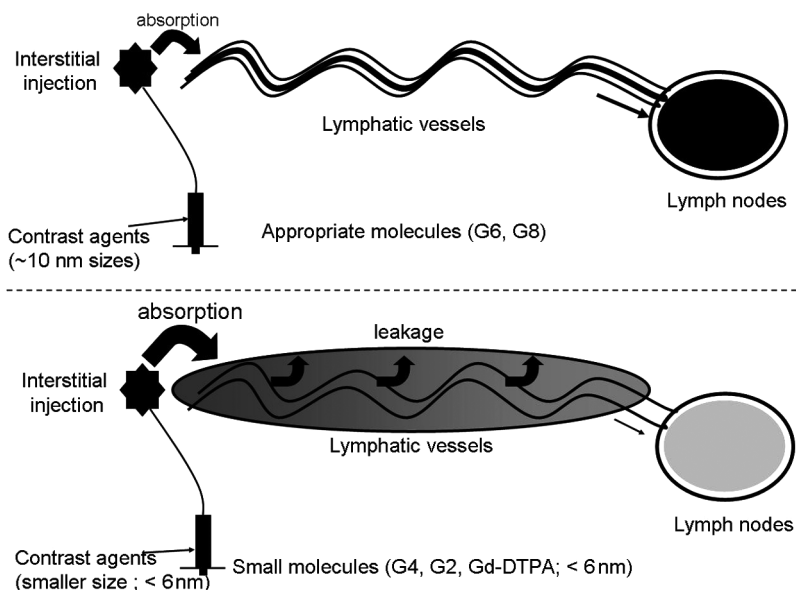


FIGURE 2.4. *Top:* G6 dendrimers are taken up by lymphatics and retained within the lymphatics resulting in opacification of the lymph nodes (black). Lower molecular weight contrast agents (*bottom*) are absorbed by the lymphatics, but leak out from them resulted in lower lymph node concentrations (gray).

The use of agents with appropriate sizes enables us to clearly depict systemic or local lymphatic vessels and lymph nodes in normal mice.

2.4.2. *Injection Routes: Intradermal vs. Subcutaneous*

Interestingly, we observed that when we injected the nano-sized contrast agents at different depths from the skin surface, the visualization of lymphatic system was affected. Intradermal injections of contrast agents visualized the lymphatics more quickly and with more signal intensity than deeper subcutaneous injections (Figure 2.5) (Kobayashi et al., 2003a). This may partially explain why sentinel lymph node imaging of the breast cancer using the intramammary gland (peri-tumoral; subcutaneous) injection required smaller agents and larger doses than systemic lymphangiography using intracutaneous injection into the skin (Kobayashi et al., 2006). As an alternative way of injecting lymphatic imaging agents for sentinel node detection, the intradermal areolar or subareolar injection has recently been proposed and used for the breast cancer growing in any location (Kern, 2001). The intradermal areola injection might decrease the required dose of contrast agent, time of imaging, and allow the use of larger agents. Still, areola injection is technically difficult in the mouse, because of the small size of the nipple compared to the needle.

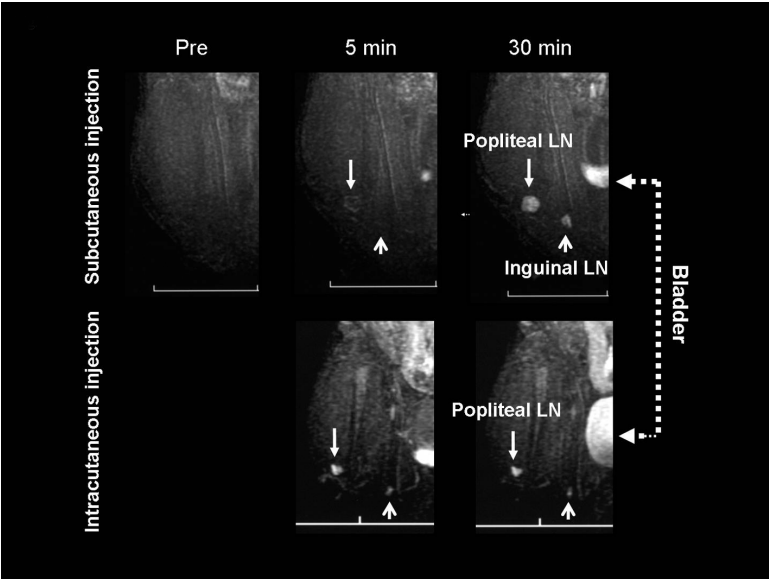


FIGURE 2.5. Dynamic MR lymphangiograms with G6 contrast agent injected into the foot either subcutaneously or intracutaneously. Intracutaneous injection showed more rapid and more intense uptake in both popliteal and inguinal LNs compared to subcutaneous injection.

## 2.5. Application of MR Lymphangiography with Nano-Sized Contrast Agents for Disease Models

### 2.5.1. Anatomic Abnormalities

MR lymphangiography has been tested in a variety of animal models of diseases. For instance, MR lymphangiography with Gd-dendrimer contrast agents was able to depict the location of intranodal lymphomatous infiltration similarly to direct X-ray lymphangiography (Figure 2.6). Although involvement of lymphoma rarely blocked the lymphatic flow, lymph node metastasis of solid cancers blocked the lymphatic flow. When this occurred, MR lymphangiography could detect the collateral lymphatic flow bypassing the blocked lymph node (Figure 2.7) (Kobayashi et al., 2003a). In addition, this method was also able to distinguish between the appearance of infection-induced hyperplasia of lymphocytes within lymph nodes from either chronic lymphoproliferative or neoplastic conditions (Kobayashi et al., 2003c). The enhanced resolution of this method might have wide applicability to the study of immunology and cancer in both experimental animal models and clinical medicine. Additionally, since a very small dose of the agent allowed visualization of the entire deep lymphatic system, this result suggests that this application might be feasible for human use.

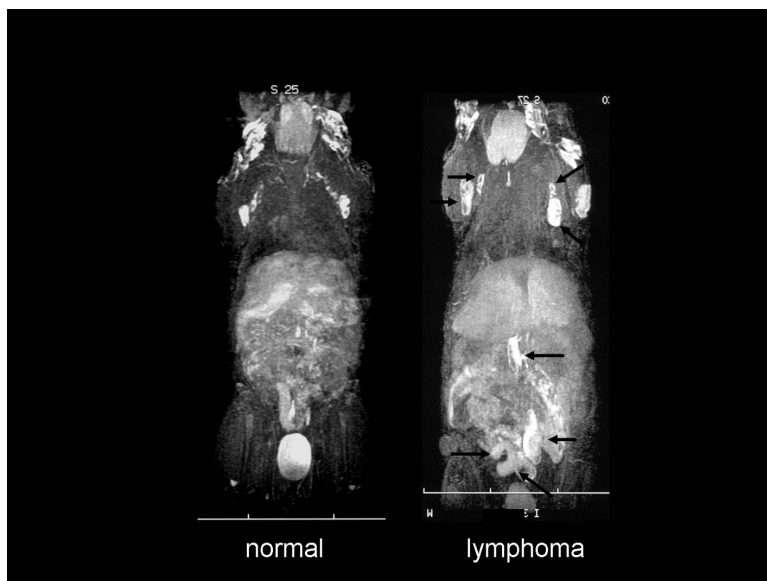


FIGURE 2.6. Whole body 3D-MR lymphangiography (MIP) of a normal or an IL-15 transgenic, lymphoproliferative/lymphoma model mouse obtained with G8 contrast agents (arrows indicate abnormal lymph nodes swelling).

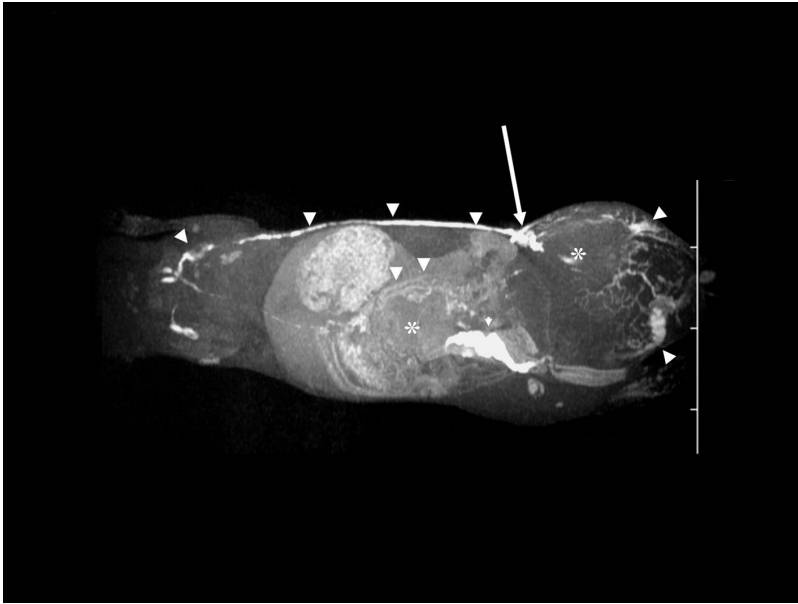


FIGURE 2.7. Whole body 3D-micro-MR lymphangiography of mice with lymph node metastasis of MC-38 cells injected with G8 agent. Large inguinal and abdominal tumors (asterisks) accompanied by a normal left inguinal lymph node (long arrow) are seen. In addition, dilated lymphatic vessels surrounding the tumor and collateral lymphatic vessels, which communicate with the thoracic duct via the axillary lymph node, are depicted (arrowheads).

### 2.5.2. *Functional Abnormalities*

In the case of lymphedema where lymphatic malformations alter lymphatic drainage patterns, the lymphatic flow may be slowed down. Currently, lymphoscintigraphy is the only clinically available method to examine lymphatic function. However, the poor spatial resolution of lymphoscintigraphy does not allow it to be applied to small animals. Even in humans, spatial resolution is inadequate to identify specific lymphatic vessels. In k-cycline transgenic mice, a lymphedema model, the dynamic MR lymphangiogram with a Gd-dendrimer contrast agent was able to diagnose the slowed lymphatic flow characteristics of lymphedema (Figure 2.8) (Sugaya et al., 2005). Another potential clinical application of MR lymphangiography is to investigate the lymphatic function of the sentinel node, which may provide insight into lymphatic flow from cancer tissue to the regional lymph nodes. For this application, the dose might be further minimized for specific local use to detect sentinel nodes metastasis of breast cancer (Figure 2.9a) (Kobayashi et al., 2004). Studies in animals were able to demonstrate detection of multiple lymph nodes, normal flow, and the lymphatic vessels as well. Nodal metastases were detectable as filling defects within the nodes. Thus, MRL using G6 dendrimer could be useful for staging, monitoring,

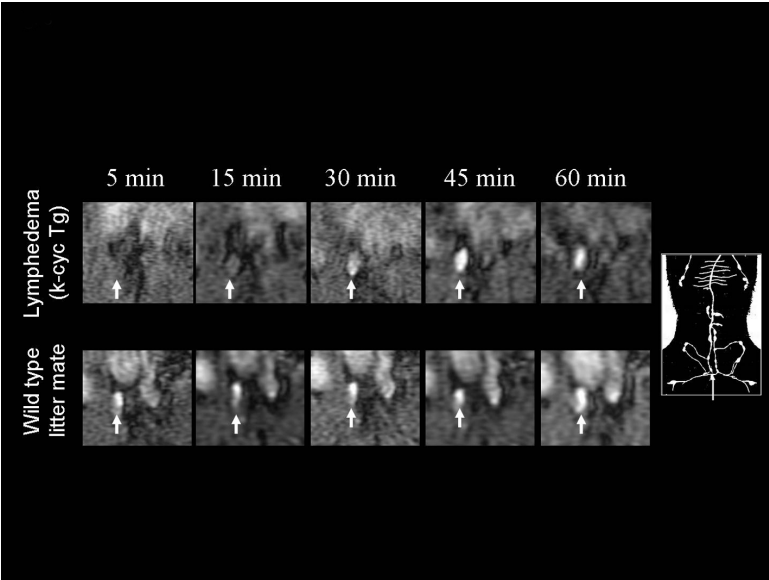


FIGURE 2.8. Dynamic MR lymphangiograms of the G8 agent showed delayed detection of the right external iliac node (arrows) in a lymphedema model mouse (k-cycline transgenic; *upper*), compared to a wild-type littermate (*lower*).

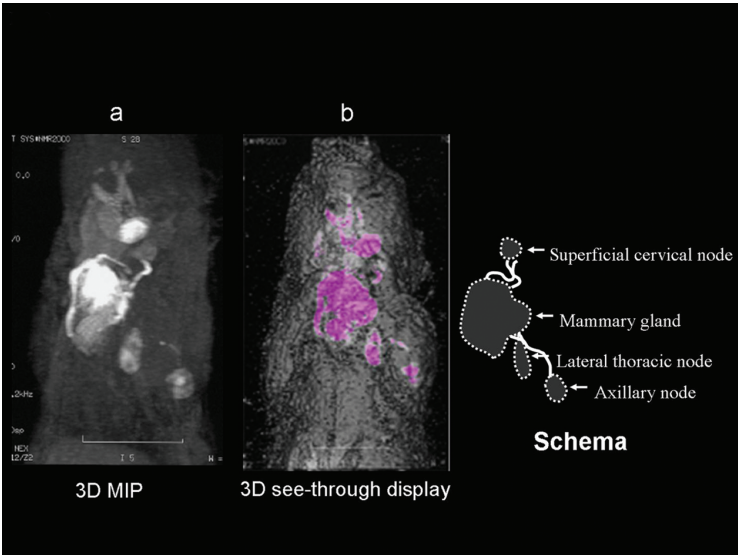


FIGURE 2.9. A chest 3D-MR mammo-lymphangiogram (maximum intensity projection; left anterior oblique view 30°) of a normal mouse obtained with G6 contrast agent at 30 min post-intramammary glands (\*) injection clearly depicts draining (sentinel) lymph nodes. 3D see-through display demonstrates the location of lymphatic vessels and sentinel lymph nodes through the skin (3D volume rendering image).

and planning surgical interventions in breast cancer patients to achieve medical and cosmetic objectives. Additionally, serial 3D images of the lymph system can be processed and presented using surface rendering to create a see-through surface (skin) in which the relation of the underlying SLN to the skin surface could be determined (Figure 2.9b).

## 2.6. Conclusion

A brief description of the preparation of Gd-dendrimer nano-size paramagnetic contrast agents has been presented, with its optimization based on the size, the possible influence of injection depth, and an overview of their applications. Interestingly, the lymphatic system is exquisitely sensitive to the physical size of the contrast agent employed and the correct match of each Gd-dendrimer to the specific MRL application is important. Therefore, lymphatic imaging appears to be a good example of the successful use of nanotechnology to solve pressing issue in biology and the medicine.

*Acknowledgement.* This research was supported by the Intramural Research Program of the NIH, National Cancer Institute, Center for Cancer Research. I would like to thank to Dr. Peter L. Choyke, Molecular Imaging Program, NCI/NIH, for his editorial assistance.

## References

- Alazraki, N.P., Styblo, T., Grant, S.F., Cohen, C., Larsen, T., Aarsvold, J.N. 2000. Sentinel node staging of early breast cancer using lymphoscintigraphy and the intraoperative gamma-detecting probe. *Semin Nucl Med* 30, 56–64.
- Alazraki, N.P., Styblo, T., Grant, S.F., Cohen, C., Larsen, T., Waldrop, S., Aarsvold, J.N. 2001. Sentinel node staging of early breast cancer using lymphoscintigraphy and the intraoperative gamma detecting probe. *Radiol Clin North Am* 39, 947–956.
- Bass, S.S., Cox, C.E., Ku, N.N., Berman, C., Reintgen, D.S. 1999. The role of sentinel lymph node biopsy in breast cancer. *J Am Coll Surg* 189, 183–194.
- Bryant, L.H., Jr., Brechbiel, M.W., Wu, C., Bulte, J.W., Herynek, V., Frank, J.A. 1999. Synthesis and relaxometry of high-generation ( $G=5, 7, 9$ , and  $10$ ) PAMAM dendrimer-DOTA-gadolinium chelates. *J Magn Reson Imaging* 9, 348–352.
- Dowlatsahi, K., Fan, M., Snider, H.C., Habib, F.A. 1997. Lymph node micrometastases from breast carcinoma: reviewing the dilemma. *Cancer* 80, 1188–1197.
- Fisher, B., Bauer, M., Wickerham, D.L., Redmond, C.K., Fisher, E.R. 1983. Relation of number of positive axillary nodes to the prognosis of patients with primary breast cancer. An NSABP update. *Cancer* 52, 1551–1557.
- Fujimoto, Y., Okuhata, Y., Tyngi, S., Namba, Y., Oku, N. 2000. Magnetic resonance lymphography of profundus lymph nodes with liposomal gadolinium-diethylenetriamine pentaacetic acid. *Biol Pharm Bull* 23, 97–100.
- Giuliano, A.E., Jones, R.C., Brennan, M., Statman, R. 1997. Sentinel lymphadenectomy in breast cancer. *J Clin Oncol* 15, 2345–2350.

- Goldhirsch, A., Glick, J.H., Gelber, R.D., Coates, A.S., Senn, H.J. 2001. Meeting highlights: International Consensus Panel on the Treatment of Primary Breast Cancer. Seventh International Conference on Adjuvant Therapy of Primary Breast Cancer. *J Clin Oncol* 19, 3817–3827.
- Guller, U., Nitzsche, E., Moch, H., Zuber, M. 2003. Is Positron Emission Tomography an Accurate Non-invasive Alternative to Sentinel Lymph Node Biopsy in Breast Cancer Patients? *J Natl Cancer Inst* 2003; 95: 95, 1040–1043.
- Harika, L., Weissleder, R., Poss, K., Zimmer, C., Papisov, M.I., Brady, T.J. 1995. MR lymphography with a lymphotropic T1-type MR contrast agent: Gd-DTPA- PGM. *Magn Reson Med* 33, 88–92.
- Kern, K.A. 2001. Breast lymphatic mapping using subareolar injections of blue dye and radiocolloid: illustrated technique. *J Am Coll Surg* 192, 545–550.
- Kobayashi, H., Brechbiel, M.W. 2003. Gadolinium-based macromolecular MRI contrast agents. *Mol Imag* 2, 1–10.
- Kobayashi, H., Brechbiel, M.W. 2004. Dendrimer-based nanosized MRI contrast agents. *Curr Pharm Biotechnol* 5, 539–549.
- Kobayashi, H., Brechbiel, M.W. 2005. Nano-sized MRI contrast agents with dendrimer cores. *Adv Drug Deliv Rev* 57, 2271–2286.
- Kobayashi, H., Kawamoto, S., Bernardo, M., Brechbiel, M.W., Knopp, M.V., Choyke, P.L. 2006. Delivery of gadolinium-labeled nanoparticles to the sentinel lymph node: comparison of the sentinel node visualization and estimations of intra-nodal gadolinium concentration by the magnetic resonance imaging. *J Control Release* 111, 343–351.
- Kobayashi, H., Kawamoto, S., Brechbiel, M.W., Bernardo, M., Sato, N., Waldmann, T.A., Tagaya, Y., Choyke, P.L. 2005. Detection of lymph node involvement in hematologic malignancies using micromagnetic resonance lymphangiography with a gadolinium-labeled dendrimer nanoparticle. *Neoplasia* 7, 984–991.
- Kobayashi, H., Kawamoto, S., Choyke, P.L., Sato, N., Knopp, M.V., Star, R.A., Waldmann, T.A., Tagaya, Y., Brechbiel, M.W. 2003a. Comparison of dendrimer-based macromolecular contrast agents for dynamic micro-magnetic resonance lymphangiography. *Magn Reson Med* 50, 758–766.
- Kobayashi, H., Kawamoto, S., Jo, S., Bryant, L.H., Jr., Brechbiel, M.W., Star, R.A. 2003b. Macromolecular MRI contrast agents with small dendrimers: pharmacokinetic differences between sizes and cores. *Bioconjug Chem* 14, 388–394.
- Kobayashi, H., Kawamoto, S., Saga, T., Sato, N., Hiraga, A., Ishimori, T., Akita, Y., Mamede, M.H., Konishi, J., Togashi, K., Brechbiel, M.W. 2001a. Novel liver macromolecular MR contrast agent with a polypropylenimine diaminobutyl dendrimer core: comparison to the vascular MR contrast agent with the polyamidoamine dendrimer core. *Magn Reson Med* 46, 795–802.
- Kobayashi, H., Kawamoto, S., Saga, T., Sato, N., Hiraga, A., Konishi, J., Togashi, K., Brechbiel, M.W. 2001b. Micro-MR angiography of normal and intratumoral vessels in mice using dedicated intravascular MR contrast agents with high generation of polyamidoamine dendrimer core: reference to pharmacokinetic properties of dendrimer-based MR contrast agents. *J Magn Reson Imag* 14, 705–713.
- Kobayashi, H., Kawamoto, S., Sakai, Y., Choyke, P.L., Star, R.A., Brechbiel, M.W., Sato, N., Tagaya, Y., Morris, J.C., Waldmann, T.A. 2004. Lymphatic drainage imaging of breast cancer in mice by micro-magnetic resonance lymphangiography using a nano-size paramagnetic contrast agent. *J Natl Cancer Inst* 96, 703–708.



- Kobayashi, H., Kawamoto, S., Star, R.A., Waldmann, T.A., Tagaya, Y., Brechbiel, M.W. 2003c. Micro-magnetic resonance lymphangiography in mice using a novel dendrimer-based magnetic resonance imaging contrast agent. *Cancer Res* 63, 271–276.
- Kobayashi, H., Saga, T., Kawamoto, S., Sato, N., Hiraga, A., Ishimori, T., Konishi, J., Togashi, K., Brechbiel, M.W. 2001c. Dynamic micro-magnetic resonance imaging of liver micrometastasis in mice with a novel liver macromolecular magnetic resonance contrast agent DAB-Am64-(1B4M-Gd)(64). *Cancer Res* 61, 4966–4970.
- Kobayashi, H., Sato, N., Hiraga, A., Saga, T., Nakamoto, Y., Ueda, H., Konishi, J., Togashi, K., Brechbiel, M.W. 2001d. 3D-micro-MR angiography of mice using macromolecular MR contrast agents with polyamidoamine dendrimer core with references to their pharmacokinetic properties. *Magn Reson Med* 45, 454–460.
- Kobayashi, H., Sato, N., Kawamoto, S., Saga, T., Hiraga, A., Haque, T.L., Ishimori, T., Konishi, J., Togashi, K., Brechbiel, M.W. 2001e. Comparison of the macromolecular MR contrast agents with ethylenediamine-core versus ammonia-core generation-6 polyamidoamine dendrimer. *Bioconjug Chem* 12, 100–107.
- Misselwitz, B., Platzek, J., Raduchel, B., Oellinger, J.J., Weinmann, H.J. 1999. Gadofluorine 8: initial experience with a new contrast medium for interstitial MR lymphography. *Magma* 8, 190–195.
- Nawaz, M.K., Hamad, M.M., Abdel-Dayem, H.M., Sadek, S., Eklof, B.G. 1990. Tc-99m human serum albumin lymphoscintigraphy in lymphedema of the lower extremities. *Clin Nucl Med* 15, 794–799.
- Perrymore, W.D., Harolds, J.A. 1996. Technetium-99m-albumin colloid lymphoscintigraphy in postoperative lymphocele. *J Nucl Med* 37, 1517–1518.
- Silvestri, R.C., Huseby, J.S., Rughani, I., Thorning, D., Culver, B.H. 1980. Respiratory distress syndrome from lymphangiography contrast medium. *Am Rev Respir Dis* 122, 543–549.
- Staatz, G., Spuntrup, E., Buecker, A., Misselwitz, B., Gunther, R.W. 2002. T1-weighted MR-lymphography after intramammary administration of Gadomer-17 in pigs. *Rofo Fortschr Geb Rontgenstr Neuen Bildgeb Verfahr* 174, 29–32.
- Suga, K., Yuan, Y., Ogasawara, N., Okada, M., Matsunaga, N. 2003. Localization of breast sentinel lymph nodes by MR lymphography with a conventional gadolinium contrast agent. Preliminary observations in dogs and humans. *Acta Radiol* 44, 35–42.
- Sugaya, M., Watanabe, T., Yang, A., Starost, M.F., Kobayashi, H., Atkins, A.M., Borris, D.L., Hanan, E.A., Schimel, D., Bryant, M.A., et al. 2005. Lymphatic dysfunction in transgenic mice expressing KSHV k-cyclin under the control of the VEGFR-3 promoter. *Blood* 105, 2356–2363.
- Tomalia, D.A., Naylor, A.M., Goddard III, W.A. 1990. Starburst dendrimers: Molecular-level control of size, shape, surface chemistry, topology, and flexibility from atoms to macroscopic matter. *Angew Chem-Int Ed* 29, 138–175.
- Torchia, M.G., Misselwitz, B. 2002. Combined MR lymphangiography and MR imaging-guided needle localization of sentinel lymph nodes using Gadomer-17. *Am J Roentgenol* 179, 1561–1565.
- Torchia, M.G., Nason, R., Danzinger, R., Lewis, J.M., Thliveris, J.A. 2001. Interstitial MR lymphangiography for the detection of sentinel lymph nodes. *J Surg Oncol* 78, 151–156.
- Veronesi, U., Galimberti, V., Zurrada, S., Pigatto, F., Veronesi, P., Robertson, C., Paganelli, G., Sciascia, V., Viale, G. 2001. Sentinel lymph node biopsy as an indicator for axillary dissection in early breast cancer. *Eur J Cancer* 37, 454–458.



- Wiener, E.C., Brechbiel, M.W., Brothers, H., Magin, R.L., Gansow, O.A., Tomalia, D.A., Lauterbur, P.C. 1994. Dendrimer-based metal chelates: a new class of magnetic resonance imaging contrast agents. *Magn Reson Med* 31, 1–8.
- Wu, C., Brechbiel, M.W., Kozak, R.W., Gansow, O.A. 1994. Metal-chelate-dendrimer-antibody constructs for use in radioimmunotherapy and imaging. *Bioorg Med Chem Lett* 4, 449–454.
- Yordanov, A.T., Kobayashi, H., English, S.J., Reijnders, K., Milenic, D., Krishna, M.C., Mitchell, J.B., Brechbiel, M.W. 2003. Gadolinium-labeled dendrimers as biometric nanoprobe to detect vascular permeability. *J Mater Chem* 13, 1523–1525.

Nanoparticles in Biomedical Imaging

Emerging Technologies and Applications

Bulte, J.W.M.; Modo, M. (Eds.)

2008, XVIII, 524 p. 168 illus., 71 illus. in color.,

Hardcover

ISBN: 978-0-387-72026-5